Structural Engineering and Mechanics, *Vol. 75, No. 3 (2020) 389-399*
DOI: https://doi.org/10.12989/sem.2020.75.3.389

Seismic performance of RC frame structures strengthened by HPFRCC walls

Hyun-Do Yun[1a], Jin-Ha Hwang[2b], Mee-Yeon Kim[3c], Seung-Ho Choi[2d], Wan-Shin Park[4e] and Kang Su Kim*[2]

[1]*Department of Architectural Engineering, Chungnam National University, 99 Daehak-ro, Yuseong-gu, Daejeon 34134, Republic of Korea*
[2]*Department of Architectural Engineering, University of Seoul, 163 Seoulsiripdae-ro, Dongdaemun-gu, Seoul 02504, Republic of Korea*
[3]*Architectural 2 Part, Design Development Team, MIDAS IT, 17 Pangyo-ro 228 beon-gil, Bundang-gu, Seongnam-si, Gyeonggi-do 13487, Republic of Korea*
[4]*Department of Construction Engineering Education, Chungnam National University, 99 Daehak-ro, Yuseong-gu, Daejeon 34134, Republic of Korea*

(Received July 4, 2019, Revised February 14, 2020, Accepted March 12, 2020)

Abstract. An infill wall made of high-performance fiber-reinforced cementitious composites (HPFRCC) was utilized in this study to strengthen the reinforced concrete (RC) frame structures that had not been designed for seismic loads. The seismic performance of the RC frame structures strengthened by the HPFRCC infill walls was investigated through the experimental tests, and the test results showed that they have improved strength and deformation capabilities compared to that strengthened by the RC infill wall. A simple numerical modeling method, called the modified longitudinal and diagonal line element model (LDLEM), was introduced to consider the seismic strengthening effect of the infill walls, in which a section aggregator approach was also utilized to reflect the effect of shear in the column members of the RC frames. The proposed model showed accurate estimations on the strength, stiffness, and failure modes of the test specimens strengthened by the infill walls with and without fibers.

Keywords: seismic performance, infill wall, shear wall, HPFRCC, LDLEM

1. Introduction

Infill wall strengthening methods have been widely applied for strengthening reinforced concrete (RC) frame structures without seismic details required in the modern building codes. (D'Ayala *et al*. 2009, Kose 2009, Altin *et al*. 2008) This is because infill wall can secure high lateral seismic resistance, and it also provide rather inexpensive and simple construction compared to other seismic strengthening methods. (Jayalekshmi and Chinmayi 2016, Parulekar *et al*. 2016, Ergun and Ates 2015, Tuken *et al*. 2017, Cismasiula and Ramos 2017) However, despite the high strength and stiffness of RC frame structures strengthened by infill walls, they typically show the shear-dominant behavioral characteristics and brittle failure modes. (Altin *et al*. 2008, Farvashany *et al*. 2008, Sánchez-Alejandre and Alcocer 2010, Lefas *et al*. 2008) In case shear walls have the aspect ratios higher than 1.0, their failure mode are also influenced by flexure. (Hidalgo *et al*. 2002, Kuang and Ho 2008, Massone *et al*. 2008, Salonikios *et al*. 1999, Sittipunt *et al*. 2001) Most of infill walls have the low aspect ratios under 1.0 because their shapes are determined by the span-to-height ratios of existing frames. In this study, to overcome such limitations, the infill wall made of high-performance fiber-reinforced cementitious composites (HPFRCC) was introduced, and thereby, the brittle failure modes of RC frame structures strengthened by the infill wall can be improved. The HPFRCC improves the residual tensile stress, post-peak behavior of concrete in compression, and crack control ability, and consequently it improves shear performances of the infill walls. (Cho *et al*. 2008, Rokugo *et al*. 2009) Cyclic loading tests were carried out on an RC frame without strengthening and the RC frame structures strengthened with HPFRCC and conventional RC infill walls. A simple analytical methodology was also proposed to assess seismic responses of RC frame structures strengthened by the infill walls.

*Corresponding author, Professor
E-mail: kangkim@uos.ac.kr
[a] Professor
E-mail: wiseroad@cnu.ac.kr
[b] Post-doctoral Researcher
E-mail: jinhahwang@uos.ac.kr
[c] Assistant Manager
E-mail: kmy0315@midasit.com
[d] Post-doctoral Researcher
E-mail: ssarmilmil@uos.ac.kr
[e] Professor
E-mail: salshin@cnu.ac.kr

2. Experimental program

2.1 Specimens and test apparatus

Three RC frame specimens with non-seismic details were fabricated in this study as illustrated in Fig. 1. All the

http://www.techno-press.com/journals/sem&subpage=7
ISSN: 1225-4568 (Print), 1598-6217 (Online)

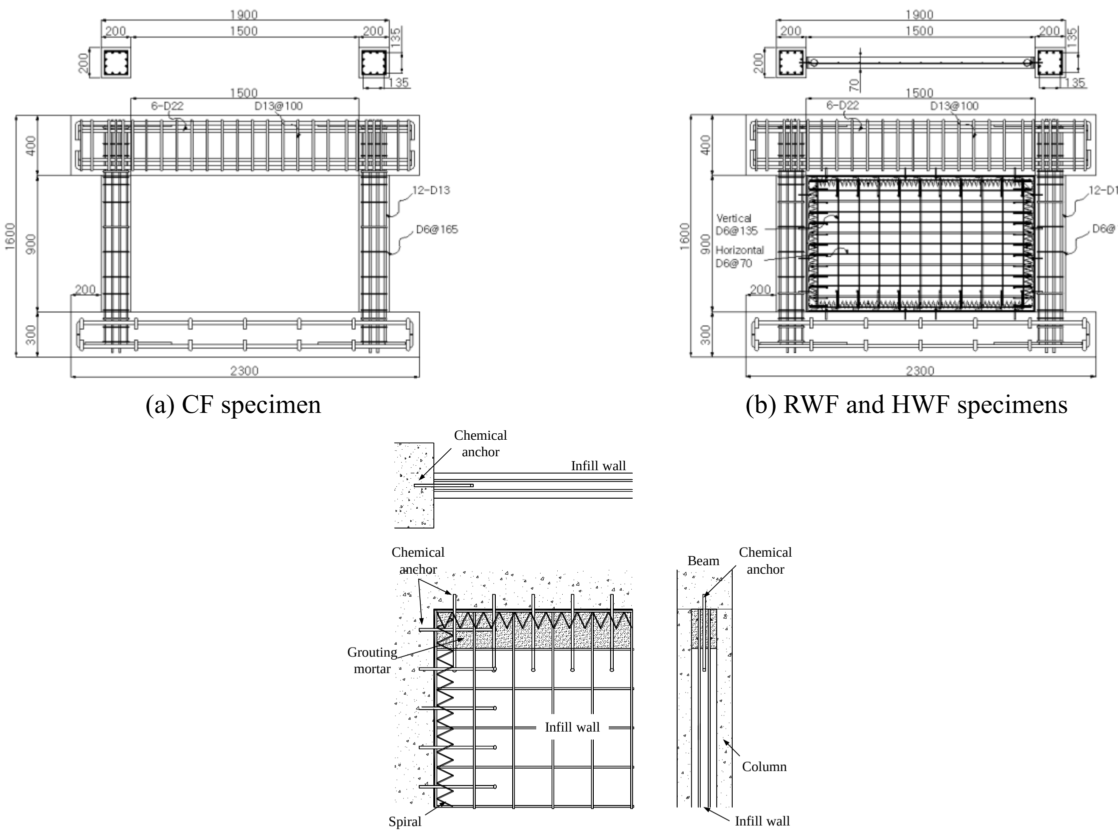

(a) CF specimen (b) RWF and HWF specimens

(c) Connection details of RWF and HWF specimens

Fig. 1 Details of test specimens

specimens were manufactured as a one-third scale because of the capacity of loading apparatus. The prototype structure was not designed against seismic loads because there was no design code that requires seismic design at the time of construction. Note that the seismic design was introduced to KCI (Korean Concrete Institute) in 1987 which was adopted from ACI 318-83. This is why the RC frames did not have any sectional details against seismic loads and do not satisfy the current seismic design criteria (ACI Committee 318-14) without strengthening. While the CF specimen shown in Fig. 1(a) was not strengthened, the RWF and HWF specimens shown in Figs. 1(b) and (c) were strengthened with conventional RC and HPFRCC infill walls, respectively. All the RC frames had the same dimensions and reinforcement details, as shown in Fig. 1(a). The columns had twelve longitudinal reinforcements of 13 mm in diameter and the hoop reinforcements of 6 mm in diameter at a spacing of 165 mm. As shown in Fig. 1(b), RC and HPFRCC infill walls used for the RWF and HWF specimens had the same reinforcement details, except for concrete materials; D6 reinforcing bars were provided with 70 mm spacing in transverse direction and 135 mm spacing in vertical direction, respectively. According to typical construction procedures adopted in practice, after the RC frame was fabricated, the reinforcements of the infill wall were then placed, and concrete was cast after formworks. As shown in Fig. 1(c), 13 mm adhesive chemical anchors with 0.32 % of reinforcement ratio were installed in connection regions between edge of the infill wall and inner face of the RC frame, and spiral bars were also placed between the infill wall and the RC frame to prevent a joint failure. In addition, non-shrinkage mortar grouts were cast around 200 mm of the joint between the beam and the infill wall to avoid drying shrinkage. The compressive strength of concrete (f_c') and the yield strengths of the steel reinforcements (f_y) measured from material tests are summarized in Table 1, where the dimensional details of the wall and column are also provided. The yield strength of D13 and D6 reinforcements were 445 MPa and 291 MPa, respectively. The compressive strength of concrete used for the RC and the HPFRCC infill walls were 21.2 MPa and 28.4 MPa, respectively. The stress-strain curves of the concrete and HPFRCC are shown in Fig. 2, where the HPFRCC, reinforced with 0.75 % of polyethylene (PE) fibers and 0.75 % of steel fibers, showed better performances both in strength and ductility. Detailed material properties of the PE fibers and the steel fibers used in this study are shown in Table 2.

Before cyclic loading, an axial load of 282.2 kN was applied to all the test specimens, which was 10 % of axial capacity of the columns. The axial load was controlled to be kept constantly during the cyclic load testing. The lateral displacement history introduced to the specimens are shown in Fig. 3. The loading protocol commonly used in previous shear wall tests was applied, where the lateral displacement is increased by the yield displacement at each step. (Salonikios and Kappos 1999, Sittipunt *et al*. 2001, Kuang and Ho 2008) In this study, the yield displacements of the

Table 1 Dimensional details and material properties of test specimens

Name	wall				column				f_c' (MPa)	Axial load (kN)
	size (mm)	ρ_v (%)	ρ_h (%)	f_y (MPa)	size (mm)	ρ_l (%)	ρ_t (%)	f_y (MPa)		
CF		-							21.2	
RWF	1500×900×70 ($l\times h\times t$)	0.33	0.70	291 (D6)	200×200 ($B\times D$)	3.81	0.36	445 (D13)	21.2	282.2
HWF									28.4	

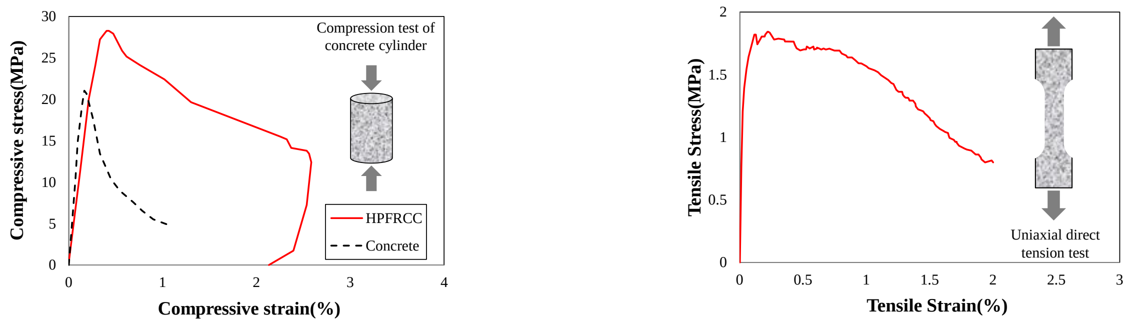

(a) Compressive stress-strain curves of conventional concrete and HPFRCC

(b) Tensile stress-strain curves of HPFRCC

Fig. 2 Stress-strain relationship of conventional concrete and HPFRCC

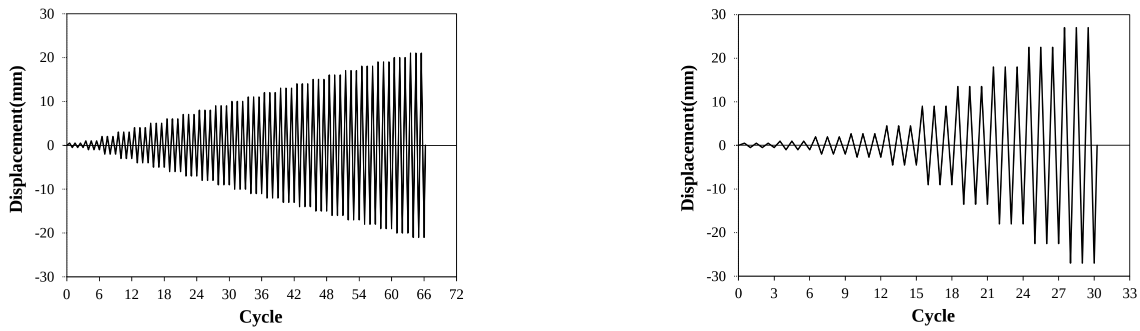

(a) CF specimen

(b) RWF and HWF specimens

Fig. 3 Cyclic loading history applied to specimens

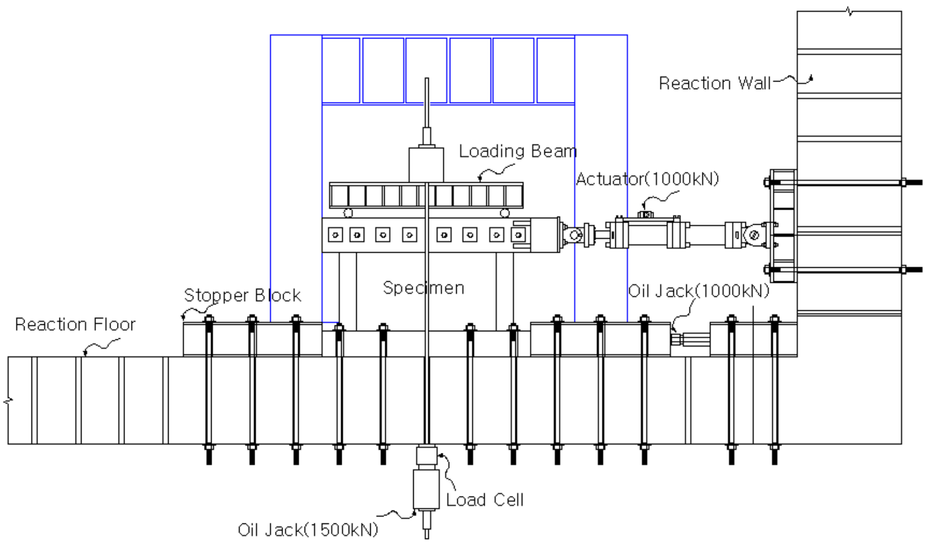

Fig. 4 Test configuration

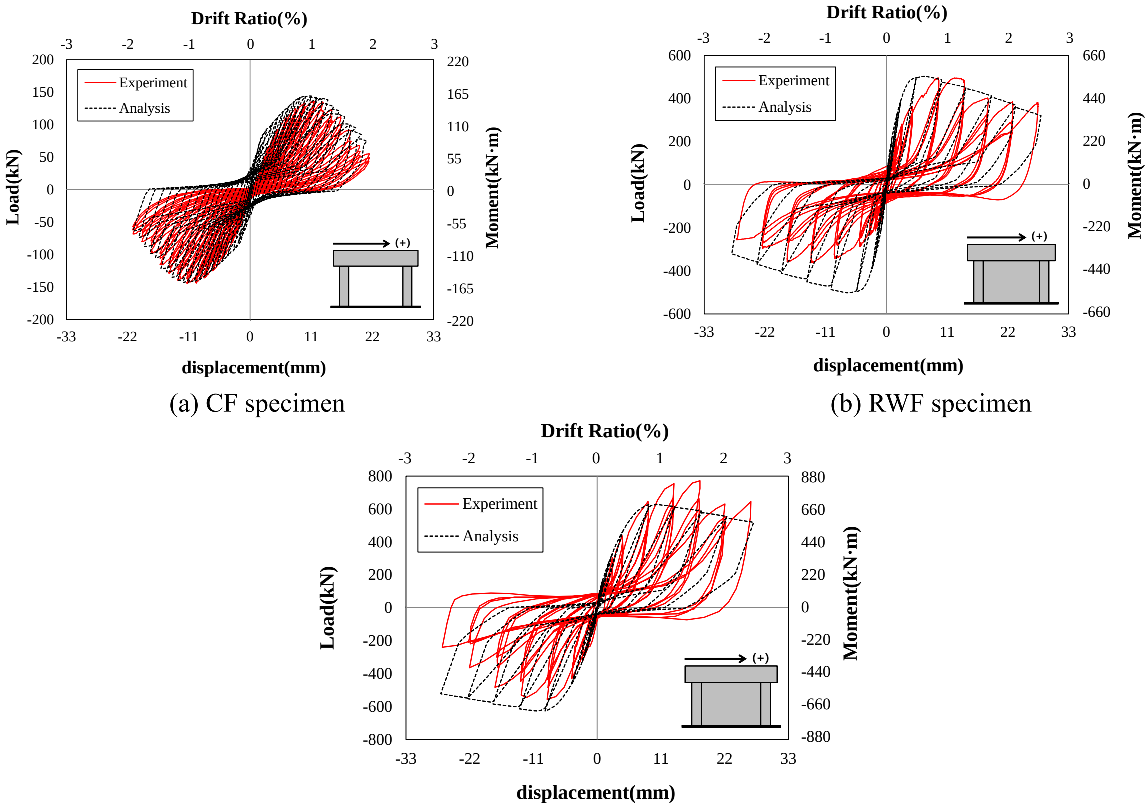

(a) CF specimen

(b) RWF specimen

(c) HWF specimen

Fig. 5 Measured and estimated load-displacement responses of test specimens

Table 2 Fiber properties

Fiber type	Unit weight (ton/m^3)	Length(mm)	Diameter(μm)	Tensile strength (MPa)
Polyethylene (PE)	0.97	15	12	2,500
Steel Fiber (SF)	7.85	32	105	2,300

non-strengthening and strengthening specimens were different, so were their loading protocols. The CF specimen with non-seismic details was expected to yield at a small displacement, and consequently the lateral load would decrease rapidly after yielding. For this reason, the displacements were increased by 1.0 mm at each loading cycle until its failure. On the other hand, for the RWF and HWF specimens strengthened with the infill walls, lateral displacements were increased by 1.0 mm till the expected yielding point, and thereafter it was increased by 4.5 mm. In addition, all the specimens were repeatedly loaded for 3 times at a same displacement level to assess the strength degradation during the cyclic test, and the test set-up of the specimens are shown in Fig. 4.

2.2 Experimental results and observations

The load-displacement responses of the CF, RWF, and HWF specimens obtained from cyclic loading tests are shown in Fig. 5. The CF specimen showed nonlinear behavior after the cracking and the load increased steadily to a maximum load of 140 kN at the 1.1% drift level. After peak, shear cracks were observed from the columns, and the load decreased rapidly. This failure pattern can be seen in Fig. 6(a). The RWF specimen strengthened with the conventional RC infill wall showed a maximum load of 495 kN, which was 3.5 times larger than the CF specimen without strengthening. In addition, the load did not decrease much after the maximum load, and it maintained 75 % of the maximum load up to 2.5 % drift ratio. Finally, the RWF specimen failed due to significant shear damages in the columns. The HWF specimen strengthened with the HPFRCC infill wall showed the maximum load of 769 kN, which is 5.5 times and 1.6 times greater than the CF and the RWF specimens, respectively, and the post-peak behavior was also significantly enhanced compared to the CF and the RWF specimens. The final failure was led by the spalling of concrete cover of the columns with a rapid decrease of the load. Even though the HPFRCC wall improved the strength and ductility, the damage of the columns with non-seismic details led to the failure. Regarding the failure mode, it will be discussed in the analysis section.

Based on the study by Seo *et al.* (1998), Hawkins and Ghosh (2004) proposed that the shear wall should secure 1.0 % ~ 3.0 % of minimum drift ratio at ultimate state, which can be expressed as a function of the aspect ratio (h/l), as follows:

$$1\,\% \leq \frac{\delta}{h}(\%) = 0.67\left(\frac{h}{l}\right) + 0.52 \leq 3\,\% \tag{1}$$

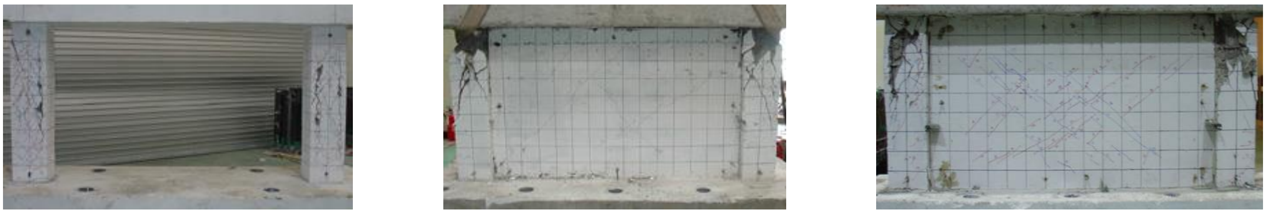

(a) CF specimen (b) RWF specimen (c) HWF specimen

Fig. 6 Crack patterns of the test specimens

where δ is the displacement at 80 % of the maximum load (i.e., $0.8P_n$) in the post-peak response, and h and l are the height and length of the shear wall, respectively. The aspect ratio of the infill wall employed in this study was 0.6, and thus test specimens should secure at least 1.0 % drift capacity according to Eq. (1). The drift ratio of the RWF specimen at $0.8P_n$ after the peak was about 2.0 %, while that of the HWF specimen was about 2.5 %. The strengthened specimens satisfied the minimum drift ratio suggested by Hawkins and Ghosh(2004), and the HWF specimen strengthened with HPFRCC also showed an enhanced deformation capacity compared to the CF specimen.

3. Numerical model

The numerical modeling of the RC frame structure strengthened with infill walls can be divided into three parts; the existing RC frame structure consisting of the column and beam member, the infill wall inserted in the RC frame, and the joint regions between the RC frame and the infill wall. In this study, the existing RC frame structure having non-seismic details was modelled using the nonlinear beam-column element (Neuenhofer and Filippou 1997, 1998, Taucer *et al*. 1991, Spacone *et al*. 1992) provided in the OpenSees program platform. One of the macro modeling methods, so-called the longitudinal and diagonal line element model (LDLEM) (Kim *et al*. 2011, Park and Eom 2007) was modified in this study and then utilized for the modeling of the infill walls. As shown in Fig. 7(a), the existing LDLEM consists of the beam member with infinite stiffness, the vertical elements, and the diagonal elements, where it is assumed that the vertical elements resist the flexure and the diagonal elements resist the shear. The diagonal elements represent the web concrete of the infill walls, which resists the shear force by both the tensile and compressive strut mechanisms. In this study, the web width of the infill wall (h_w) was determined as the region where only the tensile stresses were developed due to the lateral loading in both positive and negative directions through flexural analysis results on the infill wall section. In the existing numerical models (Otani 1974, Kabeyasawa *et al*. 1983, Linde and Bachmann 1994, Vulcano and Bertero 1987) the moment distribution in the beam-exterior column joints is different from the actual one because they were modeled as pinned connections. Therefore, in this study, the joints between the beams and the exterior columns were modeled as fixed connections, as shown in Fig. 8. For the beam column joint, it can be modelled with existing joint models (Elmorsi *et al*. 2000, Lowes *et al*. 2003), but it was excluded in this study. This is because the beams were designed very strongly for the purpose of applying lateral loads on the wall, and thus the joint shear failure did not occur. As shown in Fig. 1, a sufficient amount of the shear connectors was provided in the joints between the infill wall and the existing RC frame, and they were thus assumed to be perfectly composite, which is supported by the experimental investigations in this study; no sign of failure at the joints between the infill wall and the existing RC frame was observed in the experiments conducted in this study.

As aforementioned, the RC frame having non-seismic details (the CF specimen) was modelled using the nonlinear beam-column element (Neuenhofer and Filippou 1997, 1998, Taucer *et al*. 1991, Spacone *et al*. 1992) based on the fiber section analysis approach, and the section aggregator (McKenna *et al*. 2000) was used to consider the effect of the shear failure of the individual members on the lateral cyclic response of the whole structure. The section aggregator is a simple method to reflect the shear effect in the fiber section model, whose main concept is shown in Fig. 7(b). On this basis, the shear and flexural failure mechanisms of the beam and column members were considered in this study. The shear behavior of RC section was obtained using the modified compression field theory (MCFT) (Vecchio and Collins 1986, Bentz *et al*. 2006) and these results were then added into the fiber section analysis through the section aggregator. The confined concrete inside the hoop reinforcements in the column section was modelled with Mander's model(Mander *et al*. 1988), and the unconfined concrete outside the hoop reinforcements was modelled with the hysteretic model proposed by Yassin (1994). The Giuffré-Menegotto-Pinto Model (Filippou *et al*. 1983) was adopted for the stress-strain relationship of the steel reinforcement. For the shear response of the column members, the shear stress-strain curves obtained from the MCFT was used for the backbone curve of the Pinching 4 model (Lowes *et al*. 2003), which was combined with the fiber section model through the section aggregator. Pinching 4 material was originally developed for modeling of beam-column joint, but the pinching effect in the shear behavior was similar to the ones in the beam-column joint. (Magna and Kunnath 2012, Jeong and Jang 2016) Thus, in this study, it was used to model the shear behavior of columns. The loading/unloading stiffness and strength degradation characteristics of the Pinching 4 model, which is the key concept to consider the effect of shear in individual

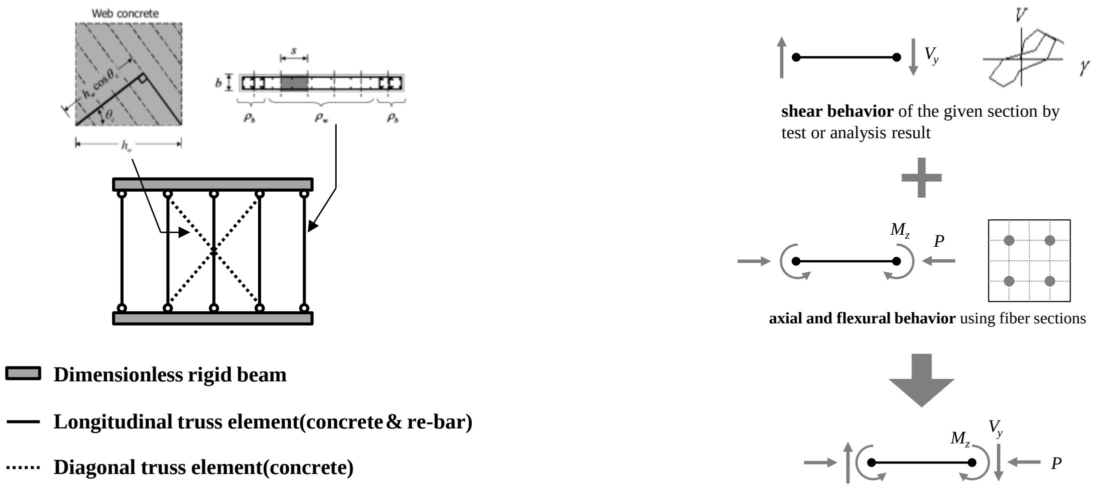

(a) LDLEM modeling (b) Section aggregator

Fig. 7 Numerical modeling for nonlinear analysis

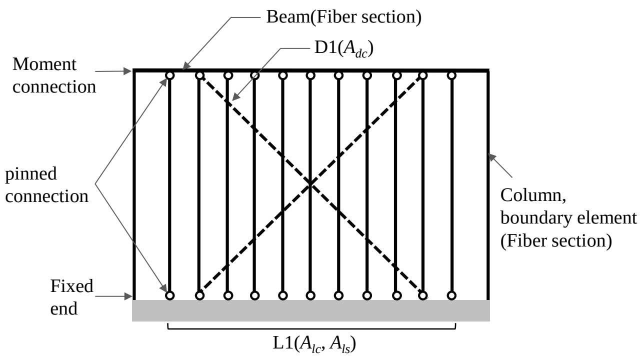

Fig. 8 Idealized numerical model of infill wall system using modified LDLEM

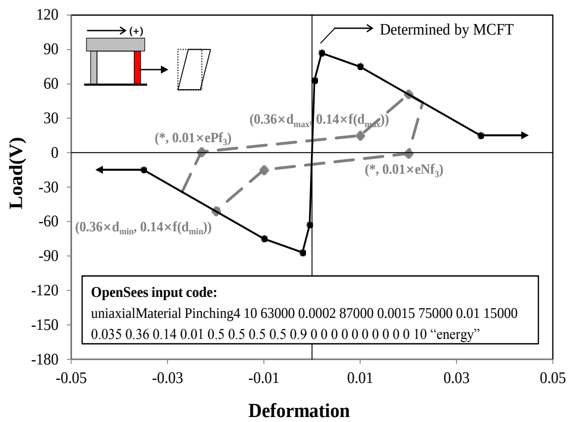

Fig. 9 Hysteretic shear behavior of reinforced concrete column

members in this study, were determined from the experimental results of the CF specimen, and the hysteretic shear behavior adopted in the section aggregator approach is illustrated in Fig. 8. For reference, the input values of the Pinching 4 model employed in this study are also presented at the bottom of Fig. 9.

The RC frames of RWF and HWF specimens were modeled in the same way done for the CF specimens as shown in Fig. 8, and the joints between the RC frame and the infill wall were assumed to be fully integrated by the sufficient connection reinforcements. The vertical and diagonal elements of the infill walls were connected to the beam by the pinned connection, and the vertical elements of the infill walls were modelled using eleven elements at the same positions of reinforcements provided in the specimens. Also, the stress-strain relationship obtained through the material test of the HPFRCC illustrated in Fig. 2(b) was modified by the Yassin model(1994). The sectional area of each element in the infill wall used in the analysis are summarized in Table3. The vertical element L1 inside the wall contained the steel reinforcements while the diagonal truss element D1 consisted of only HPFRCC or

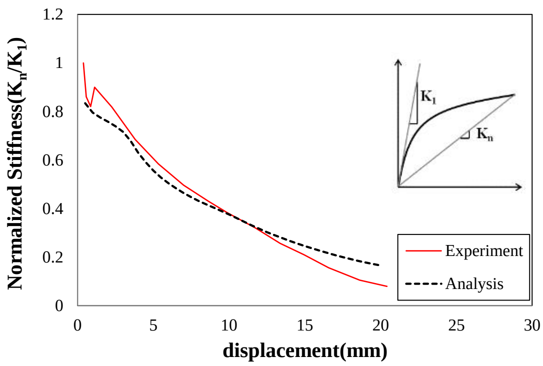

(a) CF specimen

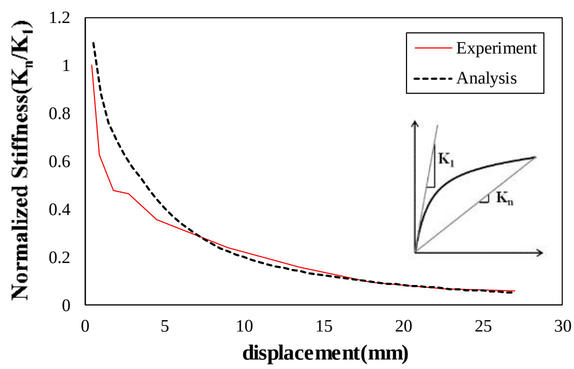

(b) RWF specimen

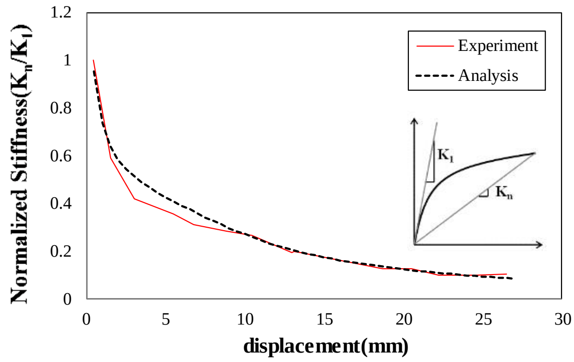

(c) HWF specimen

Fig. 10 Measured and estimate-d normalized stiffness

Table 3 Cross section area of each element of RWF and HWF specimens used in analysis

	A_{lc} or A_{dc} (mm^2)	A_{ls} (mm^2)	A_{lc}= area of longitudinal unconfined concrete A_{dc}= area of diagonal strut A_{ls}= area of longitudinal re-bars
L1	525	28.3	
D1	23,240	-	

concrete without any steel reinforcements. As shown in Fig. 8, the sectional area of each vertical element were evenly assigned, and the sectional area of diagonal element (A_{dc}) was calculated as $bh_w\cos\theta_c$ as shown in Fig. 6(a), where the thickness (b) and web width (h_w) of wall were 70 mm and 940 mm, respectively, and the inclination angle (θ_c) of 43.8° was used for the diagonal elements. The horizontal reinforcement was not modelled in this study because the contribution of horizontal reinforcement is very low in the squat shear wall.

4. Verification of numerical model

4.1 Overall cyclic responses

As shown in Fig. 5(a), the numerical model utilizing the fiber section and section aggregator approaches showed good agreements with the observed cyclic behavior of the CF specimen, and particularly, the pinching behavior due to shear was captured very precisely. In addition, as shown in Fig. 10(a) and Table 4, the numerical model accurately estimated the strength, initial stiffness, and secant stiffness changes of the CF specimen.

In Fig. 5(b), the cyclic response of the RWF specimen strengthened with the conventional RC infill wall was compared with the analysis result. While the analysis result provided a good estimation on the response in the positive direction, it showed some differences on the response in the negative direction, which showed a relatively lower strength in the experiments compared to that in the positive direction. Nevertheless, it captured the improved strength due to the strengthening by the RC infill wall well as well as the pinching behavior and the stiffness degradation of the RWF specimen. As shown in Fig. 5(c), the proposed model also estimated the strength enhancement of the HWF specimen strengthened with the HPFRCC infill wall in a good level of accuracy. As shown in Table 4, the proposed model showed good agreements with the strength and initial stiffness. The initial stiffness of the RWF specimen was greater than that of the HWF specimen in both the experimental and analysis results. This is because the elastic modulus of HPFRCC was lower than the conventional concrete due to the lack of coarse aggregate (Li 1993, Parra-Montesinos 2005, Cho *et al*. 2008).

As shown in Fig. 10(b) and (c), the reduction in stiffness of the HWF specimen was smaller than that of the RWF specimen in the initial stage. Their stiffness reduction ratio near ultimate was, however, almost the same, which is because the stiffness reduction was influenced by the damage of the columns as well as the wall and in fact the columns reached failure first. The proposed model estimated the stiffness reduction of the specimens with a good accuracy.

Table 4 Summary of test and analysis results

Specimen	Strength(kN)			Initial Stiffness(N/m)		
	Analysis	Test	Analysis/Test	Analysis	Experiment	Ratio
CF	143	141	1.01	35	37	0.95
	-142	-140	1.01			
RWF	500	495	1.01	265	245	1.08
	-502	-362	1.39			
HWF	632	769	0.82	225	236	0.95
	-627	-555	1.13			
	m=1.06, σ =0.19			m =0.96, σ =0.10		

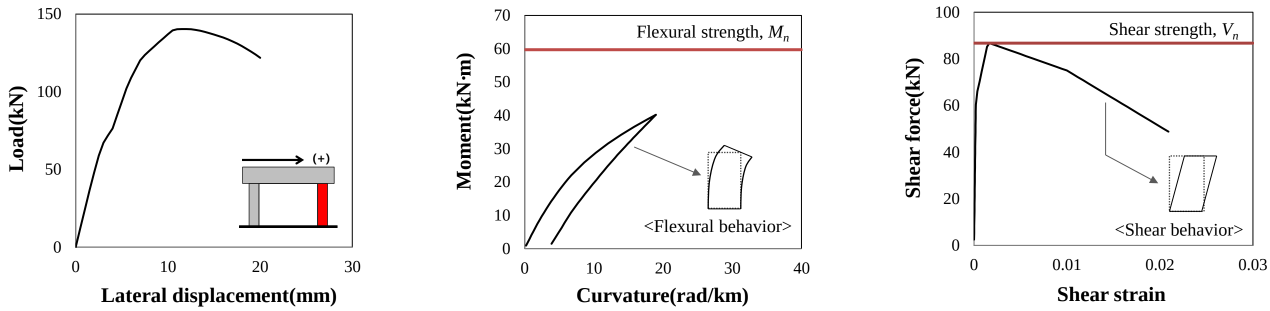

(a) Pushover (b) Flexural behavior (c) Shear behavior

Fig. 11 Flexural and shear behavior of the column element in CF specimen

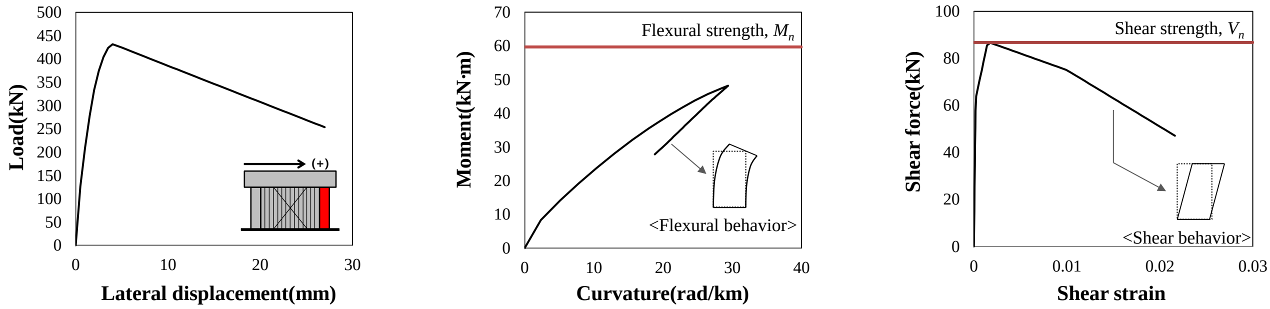

(a) Pushover (b) Flexural behavior (c) Shear behavior

Fig. 12 Flexural and shear behavior of the column element in RWF specimen

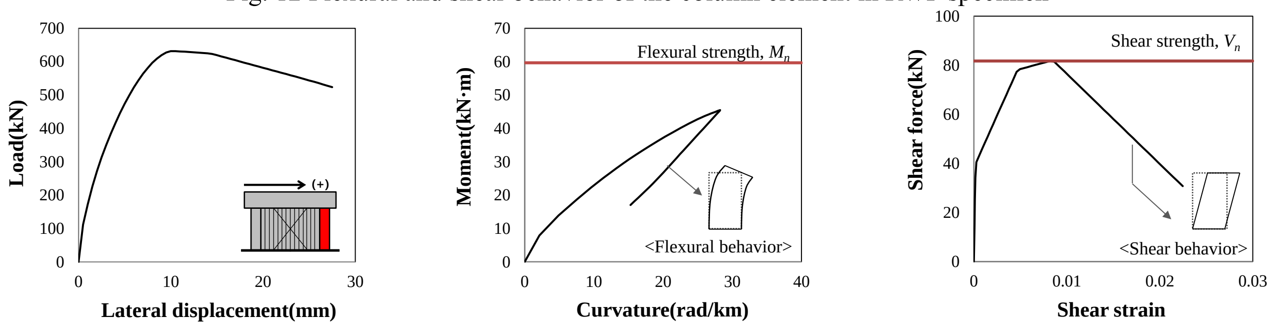

(a) Pushover (b) Flexural behavior (c) Shear behavior

Fig. 13 Flexure and shear behavior of exterior column element in HWF specimen

4.2 Failure modes

It was observed that a critical failure mode of the CF specimen without strengthening was the shear failure of the exterior column members, and the pinching phenomenon was clearly observed in the column members without seismic details. In both the test and analysis results shown in Figs. 5(b) and (c), the RWF and HWF specimens had significant strength degradations and severe pinching behaviors due to the damage in shear of the exterior column members during the unloading/reloading stages after the peak loads. In order to examine if the modified LDLEM and frame modeling method proposed in this study can assess failure modes of the test specimens properly, pushover analyses were performed as shown in Figs. 11 to

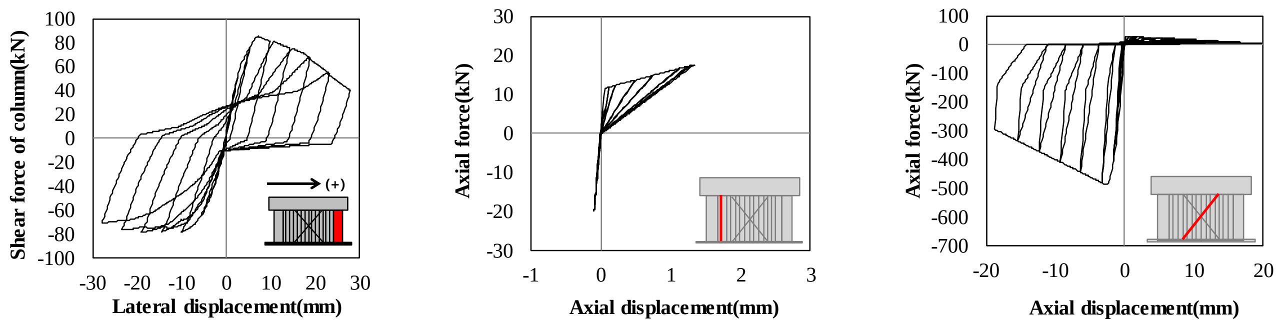

(a) boundary column (b) vertical element (c) diagonal element

Fig. 14 Estimated load-displacement responses of individual elements in RWF specimen

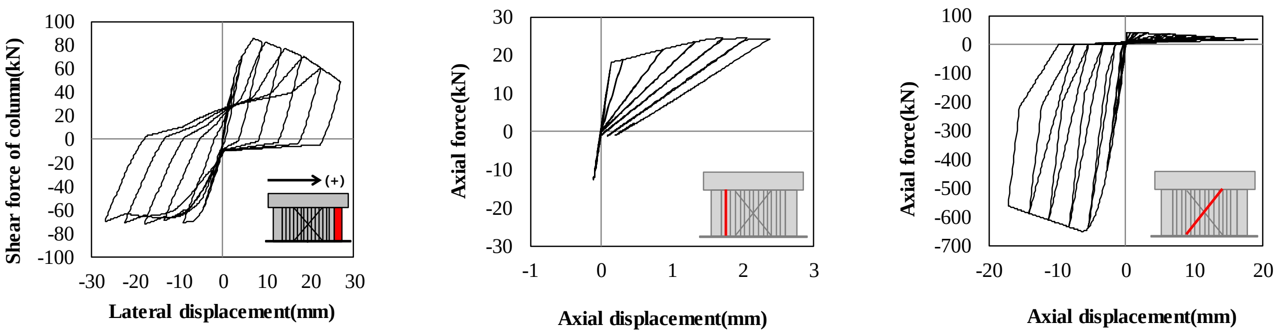

(a) boundary column (b) vertical element (c) diagonal element

Fig. 15 Estimated load-displacement responses of individual elements in HWF specimen

15. Figs. 11~13 show pushover curves of the specimens and the behavior of boundary column by dividing into the flexural and shear behavior, and Fig. 14~15 show the behavior of vertical and diagonal element under cyclic loading. It should be noted that only the analysis results were used for observation of the failure modes because no measured data is available.

Fig. 11 shows the pushover responses of the CF specimen without the infill wall as well as the moment-curvature and the shear force-strain relationship of the exterior column members. According to the moment-curvature relationship shown in Fig. 11(b), the curvatures are mostly recovered after the peak before the load reaches the flexural strength (M_n) of the column section. On the contrary, as shown in Fig. 11(c), the rapid increase in shear strains with the decrease in loading can be observed in the column member right after shear force reaches its shear capacity, which means that the exterior column member failed in shear due to its insufficient shear strength. Figs. 12 and 13 also show that the RWF and HWF specimens were dominated by the shear failure of the exterior column members similar to the CF specimen. It is worthy of mentioning that the strength degradation after the peak was less severe in the HWF specimen, compared to the CF or RWF specimens, due to the enhanced deformation capacity of the HPFRCC material used in the infill wall.

The cyclic force-displacement responses of individual elements in the RWF and HWF specimens obtained from the analysis are illustrated in Figs. 14 and 15, respectively. In Fig. 14(a), the exterior column members of the RWF specimen were modelled as the nonlinear beam-column elements, and their cyclic behavior in local coordinate system was transformed into the global lateral load-displacement relationship to directly compare their behavior with that of the whole system. In Figs. 14(b) and 14(c), since the vertical and diagonal elements in the infill walls were modelled as the uniaxial truss elements, thus their responses were expressed in the local coordinate system for convenience. In the cyclic response of the columns of RWF specimen shown in Fig. 14(a), the shear force reached the shear strength first at the right column due to the moment redistribution. As shown in Fig. 13(b), the vertical element experienced the large deformation after the yielding in tension. On the other hand, in compression, it remained within an elastic range because both the concrete and reinforcement resisted against the compression force. Since the diagonal elements shown in Fig. 14(c) were concrete elements with no steel reinforcements, their axial resistances in compression were significantly higher than those in tension and they showed softening behavior in compression after reaching their maximum compressive strengths. The maximum axial force of the diagonal elements was about 500 kN, and thus considering the inclination angle of the diagonal elements, 350 kN of the lateral load, which was about 70 % of the maximum load applied to the RWF specimen, was resisted by the diagonal elements. The rest 30 % thus appeared to be resisted by the two exterior columns. Despite the large contribution of the infill wall on the lateral strength, the shear failure occurred inevitably at the exterior columns because they had non-seismic details.

As shown in Fig. 15, the individual elements of the

HWF specimen also showed similar behavioral characteristics with those of the RWF specimen. As shown in Fig. 15(c), however, the reduction in load of the diagonal element after the peak load was less in the HWF specimen due to the fibers in tension provided in the HPFRCC infill wall. Because of this, the HWF specimen sufficiently satisfied the minimum drift ratio at ultimate presented in Eq. (1). Even in the HWF specimen strengthened with the HPFRCC infill wall, however, the shear failure of the exterior columns dominated the failure mechanism of the system because of the non-seismic details of the RC frame. Therefore, it should be clearly recognized that the reinforcement of the existing RC frame members which can secure the sufficient deformability should be preceded before the application of the infill wall strengthening method.

5. Conclusions

In this study, three RC frame specimens were fabricated and tested to investigate the seismic strengthening effects of infill walls. In addition, the non-linear numerical model was presented, where the modified LDLEM and the fiber section model were utilized and the effect of shear failure mechanism was considered using the section aggregator, and the cyclic responses of the RC frames strengthened by infill walls were evaluated. From this study, the following conclusions were drawn:

- The test specimens strengthened with the infill walls can secure the sufficient strength about 3.5 times higher than the RC frame structure without strengthening, and in particular, the RC frame specimen strengthened with the HPFRCC infill wall showed significant improvements in strength and deformation capacity.
- The HPFRCC infill wall showed small crack spacing and small crack width, thus it was considered that the HPFRCC can control the crack of the wall effectively.
- The RC frame structure having non-seismic details exhibited the shear failure in the exterior column members, and its cyclic behavior and failure mode was well estimated by the numerical model proposed in this study considering the shear behavior based on the modified compression field theory, fiber section model, and the section aggregator approach.
- The numerical nonlinear model proposed in this study accurately estimated the cyclic response and failure mode of the RC frame structures strengthened with infill walls, where the infill wall was modelled by the modified LDLEM proposed in this study.
- The analysis results of test specimens strengthened with infill walls showed that, despite that the HPFRCC reduced the degradation of axial strength of diagonal elements, there was a large strength degradation in the exterior columns of both RC and HPFRCC specimens.
- Excessive damages of RC frames were observed from the test and the analysis results of the specimens strengthened with infill walls, and it should be thus recognized that the strengthening of the existing RC frame members which can secure the sufficient deformability should be preceded before the application of the infill wall strengthening method.

Acknowledgments

This research was supported by Basic Science Research Program through the National Research Foundation of Korea (NRF) funded by the Ministry of Education (No. 2018R1A4A1025953)

References

ACI Committee 318 (1983), *Building Code Requirements for Reinforced Concrete (ACI 318-83)*, American Concrete Institute, Farmington Hills, Michigan, USA.

ACI Committee 318 (2014), *Building Code Requirements for Structural Concrete (ACI 318M-14) and Commentary*, American Concrete Institute, Farmington Hills, Michigan, USA.

Altin, S., Anil, Ö. and Kara, M. E. (2008), "Strengthening of RC nonductile frames with RC infills: An experimental study", *Cement Concrete Compos.*, **30**(7), 612-621. https://doi.org/10.1016/j.cemconcomp.2007.07.003.

Bentz, E. C., Vecchio, F. J. and Collins, M. P. (2006), "Simplified modified compression field theory for calculating shear strength of reinforced concrete elements", *ACI Mater. J.*, **103**(4), 614.

Cismasiu, C. and Ramos, A.P. (2017), "Applied element method simulation of experimental failure modes in RC shear walls", *Comput. Concrete*, **20**(6), 365-374. https://doi.org/10.12989/cac.2017.19.4.365.

Cho, C.G., Ha, G.J. and Kim, Y.Y. (2008), "Nonlinear model of reinforced concrete frames retrofitted by in-filled HPFRCC walls", *Struct. Eng. Mech.*, **30**(2), 211-223. https://doi.org/10.12989/sem.2008.30.2.211.

D'Ayala, D., Worth, J. and Riddle, O. (2009), "Realistic shear capacity assessment of infill frames: comparison of two numerical procedures", *Eng. Struct.*, **31**(8), 1745-1761. https://doi.org/10.1016/j.engstruct.2009.02.044.

Elmorsi, M., Kianoush, M. R. and Tso, W. K. (2000), "Modeling bond-slip deformations in reinforced concrete beam-column joints", *Canadian J. Civil Eng.*, **27**(3), 490-505. https://doi.org/10.1139/l99-085.

Ergun, M. and Ates, S. (2015), "The stress analysis of a shear wall with matrix displacement method", *Struct. Eng. Mech.*, **53**(2), 205-226. https://doi.org/10.12989/sem.2015.53.2.205.

Farvashany, F. E., Foster, S. J. and Rangan, B. V. (2008), "Strength and deformation of high-strength concrete shearwalls", *ACI Struct. J.*, **105**(1), 21-29.

Filippou, F. C., Bertero, V.V. and Popov, E.P. (1983), "Effects of Bond Deterioration on Hysteretic Behavior of Reinforced Concrete Joints", Report EERC 83-19; Earthquake Engineering Research Center, University of California, Berkeley.

Hawkins, N. M. and Ghosh, S. K. (2004), "Acceptance criteria for special precast concrete structural walls based on validation testing", *PCI J.*, **49**(5), 78-92.

Hidalgo, P. A., Ledezma, C.A. and Jordan, R.M. (2002), "Seismic behavior of squat reinforced concrete shear walls", *Earthq. Spectra,* **18**(2), 287-308. https://doi.org/10.1193%2F1.1490353.

Jayalekshmi, B. R. and Chinmayi, H. K. (2016), "Seismic analysis of shear wall buildings incorporating site specific ground response", *Struct. Eng. Mech.*, **60**(3), 433-453.

Jeong, S. H. and Jang, W. S. (2016), "Modeling of RC shear walls using shear spring and fiber elements for seismic performance assessment", *J. Vibroeng.*, **18**(2), 1052-1059.

Kabeyaswa, T., Shiohara, H., Otani, S. and Aoyama, H. (1983), "Analysis of the full-scale seven-story reinforced concrete test structure", *J. Faculty Eng.*, **37**(2). 431-478.

Kim, D.K., Eom, T.S., Lim, Y.J., Lee, H.S. and Park, H.G. (2011), "Macro model for nonlinear analysis of reinforced concrete walls", *J. Korea Concrete Institute*, **23**(5), 569-579. https://doi.org/10.4334/JKCI.2011.23.5.569.

Kose, M. M. (2009), "Parameters affecting the fundamental period of RC buildings with infill walls", *Eng. Struct.*, **31**(1), 93-102. https://doi.org/10.1016/j.engstruct.2008.07.017.

Kuang, J. S. and Ho, Y. B. (2008), "Seismic behavior and ductility of squat reinforced concrete shear walls with nonseismic detailing", *ACI Struct. J.*, **105**(2), 225.

Lefas, I.D., Kotsovos, M.D. and Ambraseys, N. N. (1990), "Behavior of reinforced concrete structural walls: strength, deformation characteristics, and failure mechanism", *ACI Struct. J.*, **87**(1), 23-31.

Li., V.C. (1993), "From micromechanics to structural engineering - the design of cementitious composites for civil engineering applications", *J. Struct. Mech. Earthq. Eng.*, JSCE, **10**(2), 37-48.

Linde, P. and Bachmann, H. (1994), "Dynamic modelling and design of earthquake-resistant walls", *Earthq. Eng. Struct. Dynam.*, **23**(12), 1331-1350. https://doi.org/10.1002/eqe.4290231205.

Lowes, L. N., Mitra, N. and Altoontash, A. (2003), "A Beam-Column Joint Model for Simulating The Earthquake Response of Reinforced Concrete Frames", PEER Report, Earthquake Engineering Research Center, College of Engineering University of California, Berkeley.

Magna, C. E. and Kunnath, S. K. (2012), "Simulation of nonlinear seismic response of reinforced concrete structural walls", *15th World Conference on Earthquake Engineering*, Lisbon, Portugal, September.

Mander, J. B., Priestley, M.J. and Park, R. (1988), "Theoretical stress-strain model for confined concrete", *J. Struct. Eng.*, **114**(8), 1804-1826. https://doi.org/10.1061/(ASCE)0733-9445(1988)114:8(1804).

Massone, L. M., Orakcal, K. and Wallace, J.W. (2009), "Modelling of Squat Structural Walls Controlled by Shear", *ACI Struct. J.*, **106**(5), 646-655

McKenna, F., Fenves, G. L., Scott, M. H. and Jeremic, B. (2000), *Open System for Earthquake Engineering Simulation (Opensees)*, University of California, Berkeley, USA. http://opensees.berkeley.edu.

Neuenhofer, A. and Filippou, F.C. (1998), "Geometrically nonlinear flexibility-based frame finite element", *J. Struct. Eng.*, **124**(6), 704-711. https://doi.org/10.1061/(ASCE)0733-9445(1998)124:6(704).

Neuenhofer, A. and Filippou, F.C. (1997), "Evaluation of nonlinear frame finite-element models", *J. Struct. Eng.*, **123**(7), 958-966. https://doi.org/10.1061/(ASCE)0733-9445(1997)123:7(958).

Otani, S. (1974), *A Computer Program for Inelastic Analysis of R/C Frames to Earthquake*, A Report on Research Project, (413), University of Illinois, Urbana, Champaign.

Park, H. and Eom, T. (2007), "Truss model for nonlinear analysis of RC members subject to cyclic loading", *J. Struct. Eng.*, **133**(10), 1351-1363. https://doi.org/10.1061/(ASCE)0733-9445(2007)133:10(1351).

Parra-Montesinos, G.J. (2005), "High-performance fiber-reinforced cement composites: an alternative for seismic design of structures", *ACI Struct. J.*, **102**(5), 668-675.

Parulekar, Y.M., Reddy, G.R., Singh, R.K., Gopalkrishnan, N. and Ramarao, G. V. (2016), "Seismic performance evaluation of mid-rise shear walls: Experiments and analysis", *Struct. Eng. Mech.*, **59**(2), 291-312. https://doi.org/10.12989/sem.2016.59.2.291.

Paulay, T., Priestley, M.J.N. and Synge, A.J. (1982, July), "Ductility in earthquake resisting squat shearwalls", *J. Proceedings,* **79**(4), 257-269.

Rokugo, K., Kanda, T., Yokota, H. and Sakata, N. (2009), "Applications and recommendations of high performance fiber reinforced cement composites with multiple fine cracking (HPFRCC) in Japan", *Mater. Struct.,* **42**(9), 1197-1208. https://doi.org/10.1617/s11527-009-9541-8.

Salonikios, T N. and Kappos, A.J. (1999), "Cyclic Load Behavior of Low-Slenderness Reinforced Concrete Walls: Design Basis and Test Results", *ACI Struct. J.*, **96**(4), 649-660.

Sánchez-Alejandre, A. and Alcocer, S. M. (2010), "Shear strength of squat reinforced concrete walls subjected to earthquake loading—trends and models", *Eng. Struct.*, **32**(8), 2466-2476. https://doi.org/10.1016/j.engstruct.2010.04.022.

Seo, S.Y., Lee, L.H. and Hawkins, N.M. (1998), "The limiting drift and energy dissipation ratio for shear walls based on structural testing", *J. Korea Concrete Institute*, **10**(6), 335-343. https://doi.org/10.22636/MKCI.1998.10.6.335.

Sittipunt, C., Wood, S. L., Lukkunaprasit, P. and Pattararattanakul, P. (2001), "Cyclic behavior of reinforced concrete structural walls with diagonal web reinforcement", *ACI Struct. J.*, **98**(4), 554-562.

Spacone, E., Ciampi, V. and Filippou, F.C. (1992), *A Beam Element for Seismic Damage Analysis*, Earthquake Engineering Research Center, College of Engineering, University of California, Berkeley.

Taucer, F., Spacone, E. and Filippou, F.C. (1991), *A Fiber Beam-Column Element for Seismic Response Analysis of Reinforced Concrete Structures*, Report EERC 91-17, Earthquake Engineering Research Center, College of Engineering, University of California, Berkeley.

Tuken, A., Dahesh, M.A. and Siddiqui, N.A. (2017), "Reliability assessment of RC shear wall-frame buildings subjected to seismic loading", *Comput. Concrete*, **20**(6), 719-729. https://doi.org/10.12989/cac.2017.20.6.719.

Vulcano, A. and Bertero, V. (1987), *Analytical Modeling for Predicting the Lateral Response of RC Shear Wall*, Evaluation of Their Reliability, UBC/EERC-87/19; Earthquake Engineering Research Center.

Vecchio, F.J. and Collins, M.P. (1986), "The modified compression-field theory for reinforced concrete elements subjected to shear", *ACI Struct. J.*, **83**(2), 219-231.

Yassin, M.H.M. (1994), "Nonlinear analysis of prestressed concrete structures under monotonic and cyclic loads", Ph.D. Dissertation, University of California, Berkeley.

CC